

Dependence of the specific heat of $\text{Na}_x\text{CoO}_2 \cdot y\text{H}_2\text{O}/\text{D}_2\text{O}$ on sodium and water concentrationsR. Jin,^{1,*} B. C. Sales,¹ S. Li,² and D. Mandrus^{1,2}¹Condensed Matter Sciences Division, Oak Ridge National Laboratory, Oak Ridge, Tennessee 37831, USA²Department of Physics and Astronomy, The University of Tennessee, Knoxville, Tennessee 37996, USA

(Received 1 June 2005; published 26 August 2005)

We report specific heat measurements down to 0.4 K on the layered oxide $\text{Na}_x\text{CoO}_2 \cdot y\text{H}_2\text{O}/\text{D}_2\text{O}$ with $0 \leq x \leq 0.74$ and $y=0$ and 1.4. For the nonhydrated system ($y=0$), the electronic specific heat coefficient γ_N and the Debye temperature Θ_D vary nonmonotonically with x , both displaying minima when x is close to 0.5. This indicates a systematic change of the electronic and vibrational structures with Na content. For both hydrated and deuterated systems ($x=0.35$ and $y=1.4$), the specific heat reveals a sharp peak with $\Delta C_p \sim 45.5$ mJ/mol K at $T_c^{\text{mid}} \sim 4.7$ K and an anomaly at $T_x \sim 0.8$ K. While the origin of the latter is not clear, the former corresponds to the superconducting transition. With the application of magnetic fields up to 14 Tesla, T_c decreases gradually but T_x remains more or less unchanged. The implication of these results is discussed.

DOI: 10.1103/PhysRevB.72.060512

PACS number(s): 74.25.Bt, 74.20.Rp, 74.25.Jb, 74.90.+n

There is growing evidence that the strong electron-electron correlation in layered Na_xCoO_2 is responsible for some of its anomalous physical properties such as its “colossal” thermopower^{1,2} and possibly superconductivity in its hydrated form.³ Although it is a good metal with high electrical conductivity for a wide Na-doping range except for $x=0.5$, both local-density approximation (LDA) calculations⁴ and experimental work⁵ indicate that the itinerant bands of Na_xCoO_2 are very narrow with $W \ll U$, where W is the band width and U is the effective on-site Coulomb interaction. This implies a high value of the density of states (DOS) at the Fermi level. However, all specific heat data reported so far reveal a weak or moderate enhancement of electronic specific heat coefficient γ_N for both hydrated and nonhydrated cases compared to the value from the LDA band structure.^{4,6–9} In these reports, the γ_N value was obtained by analyzing specific heat data above 2 K for x in the range of 0.3–0.8. It is possible that the extracted γ_N value does not represent that for $T \approx 0$ K. On the other hand, recent calculations, using the LDA+ U method, suggest that the strength and effect of Coulomb interactions are reduced with decreasing x .¹⁰ One would thus expect a variation of γ_N with x .

On the experimental side, the electronic properties of hydrated and nonhydrated Na_xCoO_2 have not been systematically studied as a function of composition. While the phase diagram shown in Ref. 11 is constructed from electrical transport and magnetic measurements for $1/3 \leq x \leq 3/4$ and water content $y=1.4$, little is known about how the thermodynamic properties vary with both x and y . Of particular importance is the specific heat behavior in the superconducting state of the system, which can provide key information about the superconducting pairing symmetry. In this paper, we report the low-temperature specific heat of $\text{Na}_x\text{CoO}_2 \cdot y\text{H}_2\text{O}/\text{D}_2\text{O}$ with $0 \leq x \leq 0.74$ and $y=0$ and 1.4.

Single crystals of Na_xCoO_2 were used for specific heat measurements. Starting with $\text{Na}_{0.74}\text{CoO}_2$ single crystals grown using a flux method,¹² crystals with smaller x were obtained by chemical deintercalation as described in Ref. 6. By controlling the deintercalation time, we obtain single crystals with $x \approx 0.72$ and 0.48, as determined from measurements of the c -axis lattice parameter using the calibration

curve in Ref. 11. However, it is known that the above technique cannot extract all Na from Na_xCoO_2 . In order to obtain CoO_2 ($x=0$) with the hexagonal structure, we extract all Li from LiCoO_2 powders using NO_2BF_4 as described in Ref. 13. Polycrystalline samples of $\text{Na}_{0.35}\text{CoO}_2$ and superconducting $\text{Na}_{0.35}\text{CoO}_2 \cdot 1.4\text{H}_2\text{O}/\text{D}_2\text{O}$ were prepared following a procedure similar to that described in Ref. 14. Specific heat measurements were carried out using a physical property measurement system (PPMS) from Quantum Design.

In Fig. 1(a), we present the temperature (T) dependence of the specific heat (C_p) for Na_xCoO_2 with $x \sim 0.74, 0.72, 0.48, 0.35, 0$. Note that C_p varies monotonically with T between 0.4 and 10 K and the curve tends to move upward with increasing x . For easy analysis, we replot the data as C_p/T vs T^2 as shown in Fig. 1(b). If the specific heat is due to electrons and phonons only, it is expected that C_p/T will be a linear function of T^2 at low T . While this is true for CoO_2 ($x \sim 0$) between 0.4 and 10 K, C_p/T clearly deviates from linearity below ~ 2 K for samples with $x \neq 0$. The low- T upturn indicates that an additional contribution sets in that increases with decreasing T . Similar behavior was reported previously and was attributed to a Schottky effect.⁷ Thus, for

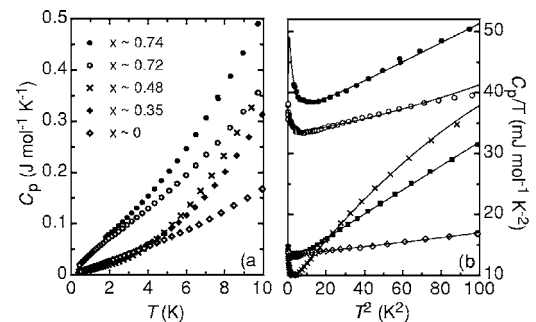


FIG. 1. (a) Temperature dependence of the specific heat C_p for single crystalline $\text{Na}_{0.74}\text{CoO}_2$ (filled circles), $\text{Na}_{0.72}\text{CoO}_2$ (unfilled circles), $\text{Na}_{0.48}\text{CoO}_2$ (crosses), polycrystalline $\text{Na}_{0.35}\text{CoO}_2$ (filled diamonds), and CoO_2 (unfilled diamonds) between 0.4 and 10 K. Shown in (b) is the replot of the data as C_p/T vs T^2 , and the solid curves are the fits of experimental data to Eq. (1).

TABLE I. Parameters obtained from the fit of experimental data between 0.4 and 10 K to Eq. (1) and the inferred Debye temperatures Θ_D (see text) for all x values.

x	γ_N (mJ/mol K ²)	β_3 (mJ/mol K ⁴)	Θ_D (K)	β_5 (μ J/mol K ⁶)	α (mJ K ² /mol)	Δ (K)
0.74	34.05	0.2051	328.2	-0.3447	258.1	3.849
0.72	32.91	0.0773	453.6	-0.0875	19.44	1.774
0.48	8.231	0.3958	257.4	-0.990	11.59	1.335
0.35	12.11	0.2002	319.0	-0.0232	3.410	1.203
~ 0	13.33	0.0333	559.1	0.0319	0.5174	1.150

$T \ll \Theta_D$ (Debye temperature), we may describe C_p using

$$C_p/T = \gamma_N + (\beta_3 T^2 + \beta_5 T^4) + \alpha \frac{e^{\Delta/T}}{T^3(1 + e^{\Delta/T})^2}. \quad (1)$$

These terms are corresponding to contributions from electrons, phonons (terms inside the bracket), and Schottky anomalies,¹⁵ respectively. Here, $\beta_3 = N(12/5)\pi^4 R \Theta_D^{-3}$ with $R = 8.314$ J/mol K and N = atomic number per formula unit, β_5 is a constant describing the anharmonic coupling, α is a constant proportional to number of two-level systems, and Δ is the energy separation between the two levels.

The solid curves shown in Fig. 1(b) are fits of experimental data between 0.4 and 10 K to Eq. (1). Note that Eq. (1) describes our experimental data well in the selected fitting range for all studied compounds. Parameters obtained from the above fitting procedure are listed in Table I. Using the relationship described above, Θ_D may be calculated from the β_3 values, and are given in Table I. In view of Table I, there are a couple of remarkable features: (1) both γ_N and β_3 (Θ_D) vary nonmonotonically with x , displaying extrema for $x \sim 0.48$; (2) α decreases with decreasing x ; (3) Δ does not vary much with x . Compared to the calculated band value of $\gamma_N = 10$ mJ/mol K² for $x > 0.5$ (Refs. 4 and 10) and 13 mJ/mol K² for $x < 0.5$,¹⁰ our γ_N values have a factor of 3 enhancement for $x > 0.48$ but are very close for $x < 0.48$. This implies that the correlation effects are moderate for $x > 0.48$ and become negligible for $x < 0.48$, in very good agreement with LDA+U calculations.¹⁰ The small γ_N value for $x \sim 0.48$ is likely related to the charge ordering reported in $\text{Na}_{0.5}\text{CoO}_2$ below 52 K.¹¹ For $\text{Na}_{0.48}\text{CoO}_2$, there may exist partial charge ordering, leading to a small γ_N value. It should also be mentioned that the γ_N for the end compound CoO_2 is nonzero, consistent with the metallic behavior reported previously.¹³ Interestingly, the variation of x in Na_xCoO_2 affects not only the DOS (reflected by γ_N) but also Θ_D with a minimum occurring at the same composition ($x \sim 0.48$) as that for γ_N . This suggests strong coupling between electrons and the lattice, and the lattice tends to soften near $x = 0.5$. The monotonic decrease of α with x reflects that the Schottky specific heat C_p^{Sch} decreases with Na content, and is almost negligible in CoO_2 . This is consistent with the trend that the low- T magnetic susceptibility decreases with decreasing x .¹¹ The almost constant Δ value for different x strongly suggests that C_p^{Sch} is mainly controlled by nuclear moments.

We now focus on the specific heat of hydrated and deuterated $\text{Na}_{0.35}\text{CoO}_2$. Shown in Fig. 2(a) is the T dependence of C_p for $\text{Na}_{0.35}\text{CoO}_2 \cdot 1.4\text{H}_2\text{O}/\text{D}_2\text{O}$ between 0.4 and 10 K. Compared to that of the parent compound, C_p of hydrated and deuterated $\text{Na}_{0.35}\text{CoO}_2$ is larger at high T but smaller below ~ 2 K. Most prominent is the specific heat anomaly below $T_c \sim 5$ K in both hydrated and deuterated cases, reflecting the superconducting phase transition. To obtain superconducting-state properties, all nonelectronic contributions, which are not affected by the superconducting phase transition, should be subtracted from the total specific heat. As shown in Fig. 2(b), C_p/T reveals more or less linear dependence with T^2 above T_c for both hydrated and deuterated compounds. This suggests that the first two terms of Eq. (1) are dominating. While the low- T upturn is absent, C_p^{Sch} may be hidden due to sharp decrease of electronic specific heat in superconducting state. For comparison, we extract the

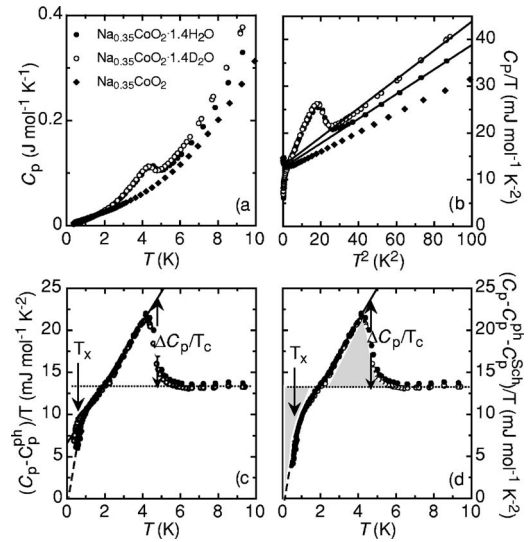


FIG. 2. (a) Temperature dependence of the specific heat C_p for polycrystalline $\text{Na}_{0.35}\text{CoO}_2 \cdot 1.4\text{H}_2\text{O}$ (filled circles), $\text{Na}_{0.35}\text{CoO}_2 \cdot 1.4\text{D}_2\text{O}$ (unfilled circles), and $\text{Na}_{0.35}\text{CoO}_2$ (filled diamonds) between 0.4 and 10 K; (b) replot of the data in (a) as C_p/T vs T^2 ; solid curves are fits of experimental data to Eq. (1); (c) and (d) present the T dependence of $(C_p - C_p^{\text{ph}})/T$ (c) and $(C_p - C_p^{\text{ph}} - C_p^{\text{Sch}})/T$ (d) of $\text{Na}_{0.35}\text{CoO}_2 \cdot 1.4\text{H}_2\text{O}$ and $\text{Na}_{0.35}\text{CoO}_2 \cdot 1.4\text{D}_2\text{O}$. In each case, the solid line is the linear fit of experimental data between 0.8 and 4.1 K and the broken line is the extrapolation of experimental data below 0.7 K to the origin.

electronic specific heat with or without considering C_p^{Sch} . Shown in Figs. 2(c) and 2(d) are the T dependence of the electronic specific heat assuming $C_p^{el} = C_p - C_p^{ph}$ [Fig. 2(c)] or $C_p^{el} = C_p - C_p^{ph} - C_p^{Sch}$ [Fig. 2(d)]. Here, parameters for C_p^{Sch} are assumed to be the same as that for $\text{Na}_{0.35}\text{CoO}_2$ (see Table I) since they cannot be determined by fitting data above T_c , and $C_p^{ph}(T)$ are obtained by fitting the experimental data between 6 and 10 K without [Fig. 2(c)] or with [Fig. 2(d)] the consideration of the Schottky effect. It turns out that the results are almost the same at high T with only a slight difference at low T . In both cases, note that the substitution of D for H has little effect on C_p^{el} as we concluded earlier in Ref. 6. As marked by the dashed line in Figs. 2(c) and 2(d), the normal-state electronic specific heat coefficient $\gamma_N = 13.7 \text{ mJ/mol K}^2$ for $\text{Na}_{0.35}\text{CoO}_2 \cdot 1.4\text{H}_2\text{O}$ and 13.3 mJ/mol K^2 for $\text{Na}_{0.35}\text{CoO}_2 \cdot 1.4\text{D}_2\text{O}$, is very close to that for the parent compound $\text{Na}_{0.35}\text{CoO}_2$ (see Table I). This is in very good agreement with a theoretical prediction that the intercalation of water into $\text{Na}_{0.35}\text{CoO}_2$ results in little change in the electronic structure.¹⁶

Although the specific heat starts to depart from the high- T behavior at 5 K and peaks at $\sim 4.1 \text{ K}$, the thermodynamic transition temperature of $\text{Na}_{0.35}\text{CoO}_2 \cdot 1.4\text{H}_2\text{O/D}_2\text{O}$ is at $T_c^{mid} \sim 4.7 \text{ K}$ where specific heat jump reaches half of the maximum. By extrapolating the low- T C_p to T_c^{mid} [see Figs. 2(c) and 2(d)], we obtain the specific heat jump $\Delta C_p \sim 45.5 \text{ mJ/mol K}$. It follows that $\Delta C_p / \gamma_N T_c^{mid} \sim 0.71$, roughly 50% of the BCS value. According to previous work, this result is compatible with (a) 50% superconducting volume fraction^{17,18} or (b) 100% superconductivity, if there exist line nodes in the superconducting pairing symmetry.^{17,19} As the C_p measurements are always carried out in high vacuum, it is possible that some $\text{H}_2\text{O/D}_2\text{O}$ is pumped out of the material thus reducing the superconducting volume fraction. For this reason, our samples were cooled rapidly to 20 K in helium gas before pumping. Thermogravimetric analysis indicates that the $\text{H}_2\text{O/D}_2\text{O}$ content y remains 1.4 after the C_p measurements. This and the fact that all other C_p measurements on either powders^{17–19} or single crystals³ result in $\Delta C_p / \gamma_N T_c^{mid}$ up to 50% of the BCS value indicate that the small ΔC_p is unlikely due to the sample quality. In the second scenario, one would expect a T^2 dependence of C_p^{el} at $T \ll T_c$, i.e., $C_p^{el}/T \propto T$.²⁰ As may be seen in Figs. 2(c) and 2(d), C_p^{el}/T varies more or less linearly with T between 0.8 and 4.1 K. The solid lines are the linear fit to the experimental data in this region. A somewhat steeper slope is obtained when the Schottky effect is considered [see Fig. 2(d)]. Unfortunately, C_p^{el}/T shows an apparent deviation from high-temperature linearity with sharper decrease below $T_x \sim 0.8 \text{ K}$, where it seems also to approach linearly to the origin as guided by the broken lines. It should be mentioned that the entropy is well balanced when the Schottky contribution is taken into account [the shaded areas above and below the dashed line in Fig. 2(d) are equal]. This strongly suggests that the sharp decrease of C_p^{el} below T_x is unlikely due to experimental error.²¹ Although the specific heat reported by Oeschler *et al.*²² was measured above 0.8 K, it was argued in Ref. 22 that the T dependence of C_p^{el} of $\text{Na}_{0.35}\text{CoO}_2 \cdot 1.4\text{H}_2\text{O}$ should behave similarly to that of MgB_2

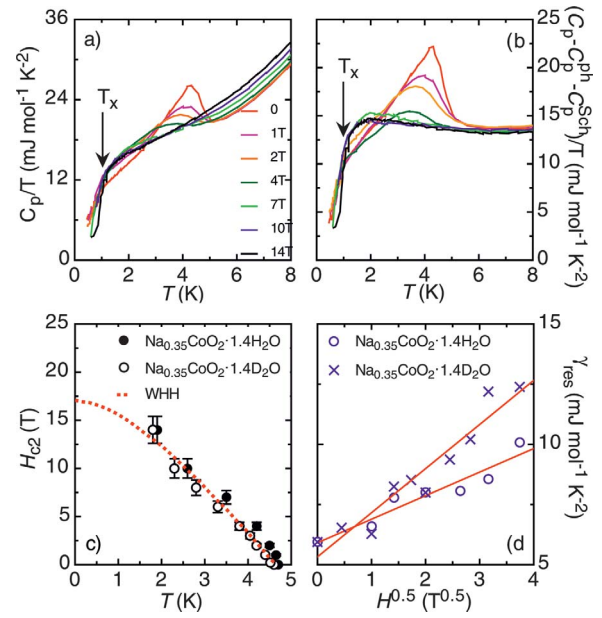


FIG. 3. (Color) Temperature dependence of C_p/T (a) and $C_p^{el}/T = (C_p - C_p^{ph} - C_p^{Sch})/T$ (b) for polycrystalline $\text{Na}_{0.35}\text{CoO}_2 \cdot 1.4\text{H}_2\text{O}$ under indicated magnetic fields; (c) T dependence of the upper critical field H_{c2} for $\text{Na}_{0.35}\text{CoO}_2 \cdot 1.4\text{H}_2\text{O}$ and $\text{Na}_{0.35}\text{CoO}_2 \cdot 1.4\text{D}_2\text{O}$. The dashed line is the fit of the data to the WHH formula; (d) H dependence of the residual electronic specific heat coefficient γ_{res} plotted as γ_{res} vs $H^{0.5}$. The solid lines are the linear fit of the data.

with two-gap superconductivity, where a sharp decrease of specific heat well below T_c is observed due to a small-gap contribution.

To gain insight into the transition at T_c and anomaly at T_x , we have measured the specific heat of $\text{Na}_{0.35}\text{CoO}_2 \cdot 1.4\text{H}_2\text{O}$ and $\text{Na}_{0.35}\text{CoO}_2 \cdot 1.4\text{D}_2\text{O}$ under the application of magnetic field. Shown in Fig. 3(a) is C_p of $\text{Na}_{0.35}\text{CoO}_2 \cdot 1.4\text{H}_2\text{O}$ plotted as C_p/T vs T with $H = 0, 1, 2, 4, 7, 10$, and 14 T . Interestingly, the anomaly at T_x seems to be insensitive to H , and remains after subtracting C_p^{ph} and C_p^{Sch} [Fig. 3(b)]. This suggests that the anomaly at T_x is unlikely due to the small-gap contribution in the two-gap superconductivity scenario.²² Similar behavior was observed in the superconducting state of single crystalline KOsO_6 ,²³ which was attributed to the dynamical instability of K ions.²⁴ To determine whether the anomaly at T_x is due to the dynamical instability of Na (which is stronger than K, according to Ref. 24) in our studied superconducting systems, further theoretical investigation is necessary.

Nevertheless, the specific heat jump due to superconducting transition weakens and moves toward lower T with increasing H , indicating the suppression of T_c and superconducting volume fraction. In Fig. 3(c), we plot the upper critical field H_{c2} vs T for polycrystalline $\text{Na}_{0.35}\text{CoO}_2 \cdot 1.4\text{H}_2\text{O/D}_2\text{O}$. Compared to that obtained from the electrical resistivity of single crystals³ and magnetic susceptibility measurements on powders,²⁵ the averaged $H_{c2}(T)$ shown in Fig. 3(c) for polycrystalline samples varies moderately with initial slope $dH_{c2}/dT|_{T_c} \sim -5.3 \text{ T/K}$. Using this value and the Werthamer-Helfand-Hohenberg (WHH) for-

mula for the dirty limit,²⁶ we may estimate the T dependence of H_{c2} between 0 and T_c . Remarkably, our experimental $H_{c2}(T)$ follows very well the WHH expression represented by the dashed line in Fig. 3(c). At $T=0$ K, the WHH formula gives $H_{c2}(0)=17.1$ T. This allows us to estimate the coherence length $\xi(0)\sim 44$ Å using $H_{c2}=\phi_0/2\pi\xi^2$ (ϕ_0 is the flux quantum). As emphasized previously,^{3,25} the coherence length is short for a superconductor with such a low T_c . On the other hand, the reduction of the superconducting volume fraction due to the application of H is reflected by the increase of γ_{res} value. From linear extrapolation of $C_p^el/T(T)$ in the linear regime of superconducting state to $T=0$ K, we obtain the intercept γ_{res} for each H and plot them as γ_{res} vs $H^{0.5}$ in Fig. 3(d) for $\text{Na}_{0.35}\text{CoO}_2\cdot 1.4\text{H}_2\text{O}/\text{D}_2\text{O}$. As guided by the solid lines, γ_{res} varies more or less linearly with $H^{0.5}$ for both systems. This is consistent with unconventional superconducting pairing symmetry with line nodes but is not a proof, since it has been seen in conventional superconductors as well.

Based on the present specific heat studies, we conclude that the electronic and vibrational properties are sensitive to x but not y in $\text{Na}_x\text{CoO}_2\cdot y\text{H}_2\text{O}/\text{D}_2\text{O}$. For the nonhydrated system with $y=0$, both γ_N and Θ_D change systematically with x , showing minima at $x\sim 0.48$. For the hydrated and deuterated system with $x=0.35$, the variation of y between 0 and 1.4 results in little effect on γ_N value. There is evidence for “double transitions” with one at $T_c\sim 4.7$ K and another at $T_x\sim 0.8$ K. While the origin of the later “transition” is not very clear, our results provide important information about the mixed-state properties due to the superconducting transition at T_c .

We thank G. M. Veith for advice on materials preparation, and D. J. Singh for fruitful discussions. Oak Ridge National Laboratory is managed by UT-Battelle, LLC, for the U.S. Department of Energy under Contract No. DE-AC05-00OR22725.

*Electronic address: jinr@ornl.gov

¹W. Koshibae, K. Tsutsui, and S. Maekawa, Phys. Rev. B **62**, 6869 (2000).

²Y. Wang, N. S. Rogado, R. J. Cava, and N. P. Ong, Nature **423**, 425 (2003).

³F. C. Chou, J. H. Cho, P. A. Lee, E. T. Abel, K. Matan, and Y. S. Lee, Phys. Rev. Lett. **92**, 157004 (2004).

⁴D. J. Singh, Phys. Rev. B **61**, 13397 (2000).

⁵B. Fisher, K. B. Chashka, L. Patlagan, A. Kanigel, A. Knizhnik, G. Bazalitsky, and G. M. Reisner, J. Phys.: Condens. Matter **15**, L571 (2003).

⁶R. Jin, B. C. Sales, P. Khalifah, and D. Mandrus, Phys. Rev. Lett. **91**, 217001 (2003).

⁷Y. Ando, N. Miyamoto, K. Segawa, T. Kawata, and I. Terasaki, Phys. Rev. B **60**, 10580 (1999).

⁸K. Miyoshi, E. Morikuni, K. Fujiwara, J. Takeuchi, and T. Hamasaki, Phys. Rev. B **69**, 132412 (2004).

⁹B. C. Sales, R. Jin, K. A. Affholter, P. Khalifah, G. M. Veith, and D. Mandrus, Phys. Rev. B **70**, 174419 (2004).

¹⁰K.-W. Lee, J. Kunes, and W. E. Pickett, Phys. Rev. B **70**, 045104 (2004).

¹¹M. L. Foo, Y. Wang, S. Watauchi, H. W. Zandbergen, T. He, R. J. Cava, and N. P. Ong, Phys. Rev. Lett. **92**, 247001 (2004).

¹²K. Fujita, T. Mochida, and K. Nakamura, Jpn. J. Appl. Phys., Part 1 **40**, 4644 (2001).

¹³S. Venkatraman and A. Manthiram, Chem. Mater. **14**, 3907 (2002).

¹⁴K. Takada, H. Sakurai, E. Takayama-Muromachi, F. Izumi, R. A.

Dilanian, and T. Sasaki, Nature **422**, 53 (2003).

¹⁵E. S. R. Gopal, *Specific Heats at Low Temperatures* (Plenum Press, New York, 1966).

¹⁶M. D. Johannes and D. J. Singh, Phys. Rev. B **70**, 014507 (2004).

¹⁷B. Lorenz, J. Cmaidalka, R. L. Meng, and C. W. Chu, Physica C **402**, 106 (2004).

¹⁸B. G. Ueland, P. Schiffer, R. E. Schaak, M. L. Foo, V. L. Miller, and R. J. Cava, Physica C **402**, 27 (2004).

¹⁹H. D. Yang, J. Y. Lin, C. P. Sun, Y. C. Kang, C. L. Huang, K. Takada, T. Sasaki, H. Sakurai, and E. Takayama-Muromachi, Phys. Rev. B **71**, 020504(R) (2005).

²⁰M. Sigrist and K. Ueda, Rev. Mod. Phys. **63**, 239 (1991).

²¹While the heat capacity of the addenda shows no anomaly at T_x , the specific heat of the sample has also been carefully examined using different methods suggested by Quantum Design. It confirms that the anomaly for the sample is not an artifact. For more information about the reliability of PPMS, see J. C. Lashley *et al.*, Crit. Rev. Plant Sci. **43**, 369 (2003).

²²N. Oeschler, R. A. Fisher, N. E. Phillips, J. E. Gordon, M. L. Foo, and R. J. Cava, Chinese J. Phys. (Taipei) (to be published).

²³Z. Hiroi, S. Yonezawa, J. I. Yamaura, T. Muramatsu, and Y. Mu-raoka, cond-mat/0502043 (unpublished).

²⁴J. Kunes, T. Jeong, and W. E. Pickett, Phys. Rev. B **70**, 174510 (2004).

²⁵H. Sakurai, K. Takada, S. Yoshii, T. Sasaki, K. Kindo, and E. Takayama-Muromachi, Phys. Rev. B **68**, 132507 (2003).

²⁶N. R. Werthamer, E. Helfand, and P. C. Hohenberg, Phys. Rev. **147**, 250 (1966).